Research on Engineering Structures & Materials
www.jresm.org
Research Group

Research Article

NiAlMo coating impact on aluminum alloy surface properties

Ali H. Naser *,a, Maryam A. Ali Bash b, A. Mezher Resen c

College of Production Engineering and Metallurgy, University of Technology, Baghdad, Iraq

Article Info

Article History:

Received 10 June 2026

Accepted 10 Aug 2026

Keywords:

NiAl Mo coating;
Plasma spraying;
Wear rate;
Microhardness

Abstract

This article explores the effects of NiAlMo coating on aluminum alloy (Al-Si). The limited hardness, inadequate wear resistance, and poor corrosion resistance of aluminum alloys restrict their broader application across various industries. The use of surface protective coatings can significantly enhance hardness and wear resistance. Plasma spraying technologies are widely utilized to improve surface properties. The results show that Vickers microhardness increased significantly from 103.7 to 347 Hv due to the application of the NiAlMo coating. Additionally, the wear rate decreased, and the scratch lines became notably finer. The coating layer acts as a barrier against oxygen penetration throughout its thickness, whereas the uncoated sample exhibited weight gain due to surface oxidation after being exposed to a furnace environment at 350°C for 50 hours.

1. Introduction

Due to advancements in science and technology, aluminum has increasingly taken the place of steel in various industries, primarily because of its lightweight properties. This transition has resulted in enhanced fuel efficiency and overall performance in vehicles and aircraft [1]. Furthermore, aluminum's resistance to corrosion makes it a compelling choice for products subjected to harsh environmental conditions [2]. Integrating corrosion resistance with excellent thermal conductivity, this material is ideal for manufacturing engine components, cylinder casings for internal combustion engines, and lightweight vehicles. These characteristics not only enhance performance but also improve overall fuel efficiency and extend the longevity of the vehicles [3, 4]. Owing to their superior castability, low density, and advantageous thermal properties, Al–Si alloys are widely utilized in automotive, aerospace, and other engineering applications, especially for engine components like pistons and cylinder heads. However, their tribological performance is crucial for their effective use under harsh service circumstances; therefore, improving surface characteristics is crucial for increasing component durability and reliability [5,6].

Notwithstanding these numerous advantages, the long-term challenges associated with this usage, particularly under harsh operating circumstances, provide difficulties for both users and developers. These problems relate to the alloy's intrinsic surface characteristics and its resilience to operational circumstances [7]. Materials produced from this substance can endure different forms of degradation under operational environments, including wear from the friction of solid particles, chemical corrosion, and thermal fluctuations that may induce alternate stresses [8]. From this perspective, enhancing their resistance was considered an important area of study. Researchers considered surface engineering by thermal spray coating techniques with important mechanical and functional properties a promising solution [9-12]. These techniques can significantly improve wear resistance and corrosion protection, leading to longer-lasting materials in various applications [13, 14].

*Corresponding author: pme.24.06@grad.uotechnology.edu.iq
aorcid.org/0009-0002-9207-6792; borcid.org/ 0000-0001-9702-118X; corcid.org/0000-0001-9312-5889
DOI: http://dx.doi.org/10.17515/resm2026-1739ma0610rs

Atmospheric plasma spraying (APS) is one of the most used thermal spray techniques for enhancing the surface characteristics of engineering materials, especially those that are subjected to extreme wear, corrosion, and high temperatures. A high-temperature plasma jet melts the feedstock material and accelerates it toward the substrate, where the molten particles quickly solidify to form a lamellar covering. The microstructure, porosity, oxide content, adhesion strength, and coating thickness all have a significant impact on the final coating performance. However, more than fifty macroscopic process parameters, such as spray distance, arc current, voltage, atomizing gas pressure, feedstock properties, and substrate preparation, affect coating quality, making APS optimization difficult. As a result, the best spraying conditions are currently mostly determined by trial and error in the manufacturing of high-quality coatings [15,16].

In addition to plasma spraying, a number of other surface modification methods, such as high-velocity oxy-fuel (HVOF) spraying, anodic oxidation [17], physical and chemical vapor deposition (PVD/CVD), laser surface treatment, and electroless coatings, have also been successfully used to enhance the performance of aluminum alloys. The necessary service conditions, coating properties, and financial factors all play a role in choosing the right method [18]. As a result, ongoing research aims to optimize these coatings for even better performance under challenging conditions. B. Shreeram et al. [19] study the effect of the implementation of Thermal Barrier Coatings (TBC) on aluminum alloy pistons utilized in internal combustion engine components considerably. La_2O_3 is blended in proportions of 10%, 20%, and 30% with mullite and plasma-sprayed onto an A356 aluminum alloy substrate, which has a base coat of NiCr. The experimental results from the tensile test and the adhesive test performed confirm that the incorporation of 10% La_2O_3 with mullite yields enhancements of 10% and 27%, respectively, and diminishes heat rejection from the combustion chamber. M. Kalyana Kumar and P. D. Sudersanan [20] employ ceramic coatings for their substantial benefits in resisting wear, corrosion, and erosion on aluminum, which is utilized in piston manufacturing. The hardness of the coated surface is increased by 37% relative to the uncoated piston material. A pin-on-disc apparatus conducted wear tests, revealing a 22% reduction in the wear rate of the coated surface compared to the uncoated surface. Corrosion test results demonstrate that the coated surface exhibits superior resistance to corrosion compared to the uncoated specimen.

This study employs thermal plasma spraying technology to enhance the properties of aluminum alloys. Metal wires composed of Ni-Al-Mo are used as the feed material to examine alterations in the surface characteristics of Al alloys, including microstructure, microhardness, phases, wear resistance, and hot corrosion resistance. The majority of research has been on ceramic coatings, HVOF-deposited layers, or traditional Ni-based systems, despite the fact that many studies have looked into thermal spray coatings for enhancing the surface performance of aluminum alloys. The application of NiAlMo wire deposited by atmospheric plasma spraying for Al–Si piston alloys has received little attention, especially when it comes to a thorough assessment of microstructure, phase evolution, microhardness, wear resistance, and hot corrosion behavior under engine operating conditions. Consequently, there is still a lack of clarity regarding the combined impact of NiAlMo coatings on certain surface properties. The application of NiAlMo wire as the coating material by atmospheric plasma spraying to concurrently enhance the mechanical and tribological performance as well as the hot corrosion resistance of an Al–Si piston alloy is what makes the current study novel. This study offers a thorough correlation between coating microstructure, phase formation, hardness increase, wear behavior, and hot corrosion resistance, in contrast to earlier studies that only concentrated on specific attributes or various coating systems. The results help to increase the possible applications of NiAlMo coatings for lightweight automotive parts that are subjected to harsh service conditions.

2. Experimental Work

A commercial diesel engine piston's hypereutectic Al–Si piston alloy served as the substrate material for this study. For microstructural analysis, hardness testing, hot corrosion testing, and coating deposition, the piston was divided into square specimens that measured 15 × 15 × 8 mm. The substrate surfaces were cleaned with ethanol to get rid of impurities after being mechanically ground using 500-grit SiC abrasive paper. In order to achieve a roughened surface that encourages mechanical interlocking and anchoring between the molten spray particles and the substrate—the main adhesion mechanism in thermal spray coatings—surface preparation was purposefully carried out. An Arc Spray System (BP400, TAFA, USA) was used to deposit the coating. The feedstock material was commercial Ni–5.5Al–5Mo wire (74MXC/Metco 8447 equivalent) with a 1.6 mm diameter. While pressurized air atomized and drove the molten droplets toward the substrate surface, the electric arc created between the two consumable wires melted the wire tips during spraying, creating a lamellar coating by quick solidification. The manufacturer's instructions and first optimization trials were used to determine the spraying settings. Table 1 summarizes the operational parameters, which were an arc voltage of 39 V, an arc current of 125 A, an atomizing air pressure of 3.8 bar, a spray distance of 200 mm, a spray angle of 90°, and a spraying period of 30 seconds. According to polished cross-sectional SEM images, the average coating thickness under these circumstances was roughly 600 ± 20 µm.

Table 1. The coating process parameters

Parameters	Value
Arc voltage	39 V
Arc current	125 A
Atomizing gas	Air
Atomizing gas pressure	3.8 bar
Spray distance	200 mm
spraying angle	90°
Spraying duration	30 s

According to the coating process, X-ray fluorescence (XRF) examination was used to determine the substrate alloy's chemical composition. Table (2) shows the elemental composition that was measured. An MTM-1A optical microscope was used to characterize the substrate's microstructure, and Scanning Electron Microscopy (SEM) with Energy Dispersive Spectroscopy (EDS) was used to analyze the morphology of the coating surface and cross-section in order to assess elemental distribution following coating and exposure to hot corrosion. X-ray diffraction (XRD) examination was used to identify the substrate's and coating's phases. A TH714 digital Vickers microhardness tester with a load of 200 g (HV0.2) and a dwell time of 15 s was used to measure the microhardness of the substrate and coating. Each specimen had five indentations made at various sites, and the given value is the average of the measurements. A pin-on-disc tribometer was used to perform dry sliding wear tests. For 20 minutes, the coated and uncoated specimens were subjected to standard loads of 5, 10, and 15 N while rotating at 490 rpm equivalent to a worn track diameter of 70 mm (7 cm) and a sliding speed of roughly 1.80 m/s. A steel disc that had been hardened made up the counter face. The specimens were dried, ultrasonically cleaned with ethanol, and weighed using an analytical balance with a resolution of 0.0001 g before and after each wear test. Three repetitions of each wear experiment were conducted, and the average result was recorded. The measured mass loss was used to compute the wear rate. The hot corrosion resistance was assessed using a molten salt mixture of 55 weight percent V_2O_5 and 45 weight percent Na_2SO_4. The specimen surface was evenly coated with around 30 mg/cm^2 of the salt mixture using kerosene as a temporary binder. In a Townson Mercer electric furnace, the coated and uncoated specimens were subjected to 350°C for 50 hours before being cooled to room temperature. In order to assess the corrosion behavior, weight variations were noted at predefined intervals. Three specimens were used for each hot corrosion test, and the given values are the mean of the three measurements.

3. Results and Discussion

3.1. Microstructural Characterization

The optical micrograph of the Al-Si alloy substrate as received is displayed in Figure (1). Eutectic silicon particles and a number of intermetallic compounds are dispersed throughout the α-Al matrix that makes up the microstructure. The XRF study (Table 2) indicates that the alloy contains about 12.3 weight percent Si, indicating a hypereutectic Al–Si alloy that is commonly used in diesel engine pistons due to its advantageous combination of low density, excellent thermal conductivity, and adequate wear resistance. However, its resilience to extreme friction and high-temperature service conditions is limited by the relatively soft aluminum matrix. Figure (2a) displays the SEM surface morphology of the plasma-sprayed NiAlMo coating.

Table 2. Chemical composition of Al-Si alloy based on XRF results

Element%	Al	Si	Mg	Cu	Fe	Mn	Zn
Content	83.9	12.3	1.2	1.1	0.56	0.39	0.27

The coating has the distinctive lamellar microstructure that is frequently seen in metallic coatings blasted with atmospheric plasma. When the molten droplets hit the substrate during spraying, they quickly flatten, creating overlapping splats that result in a dense layer with little porosity. Additionally visible are isolated micro-pores and small unmelted particles, which are common characteristics of thermally sprayed coatings and are mostly related to the fast solidification process and particle flight circumstances. A continuous NiAlMo coating layer with an average thickness of about 600 μm is shown in the cross-sectional SEM image in Figure (2b). The coating exhibits a relatively continuous lamellar structure formed by the successive deposition and rapid solidification of the sprayed particles. The coating/substrate interface is clearly distinguishable, with no obvious large-scale interfacial gaps or delamination observed in the examined cross-section. This cross-sectional morphology provides an appropriate microstructural basis for the subsequent improvement in hardness, wear resistance, and hot corrosion behavior.

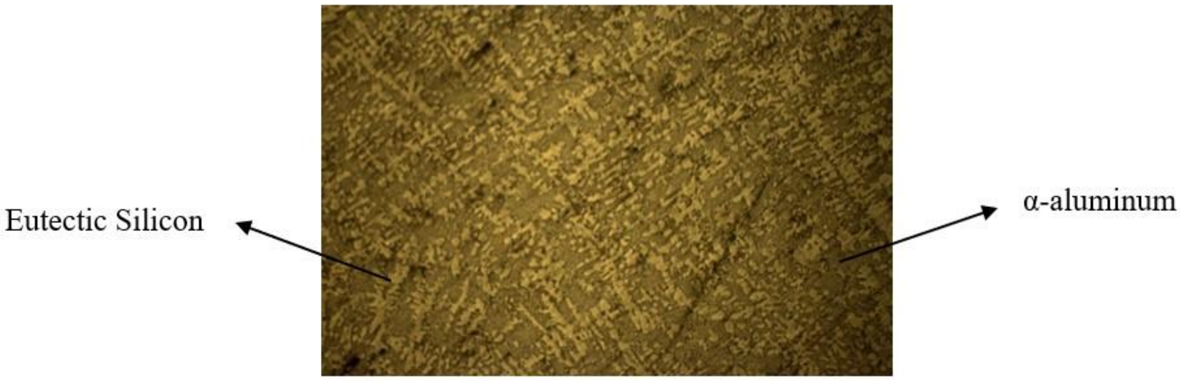

Fig. 1. Optical micrograph showing the microstructure of the Al alloy used in this study

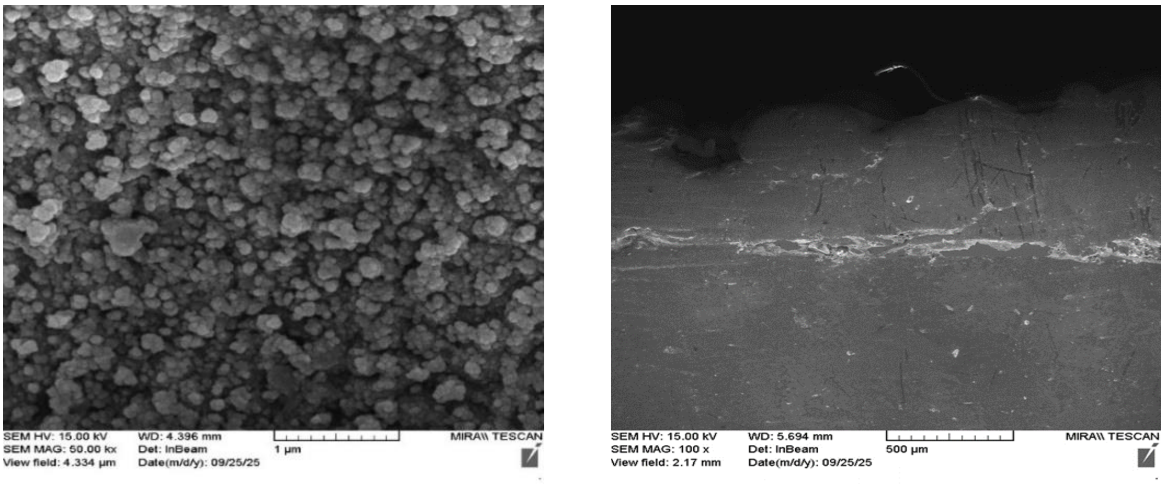

(a) (b)

Fig. 2. SEM micrograph of the (a) plan view upper surfaces of plasma-sprayed NiAlMo coating (b) cross section of plasma-sprayed NiAlMo coating

3.2. XRD Analysis

The X-ray diffraction (XRD) patterns of the substrate alloy and the plasma-sprayed NiAlMo coating are displayed in Figs. 3(a) and 3(b), respectively. XRD analysis was used to identify the crystalline phases that formed before and after the coating procedure and to evaluate the phase evolution caused by the high-temperature plasma spraying approach. The hypereutectic Al–Si composition found by the XRF analysis is confirmed by the substrate's diffraction pattern (Fig. 3a), which is dominated by prominent diffraction peaks corresponding to the α-Al matrix and complemented by distinctive peaks of crystalline Si.

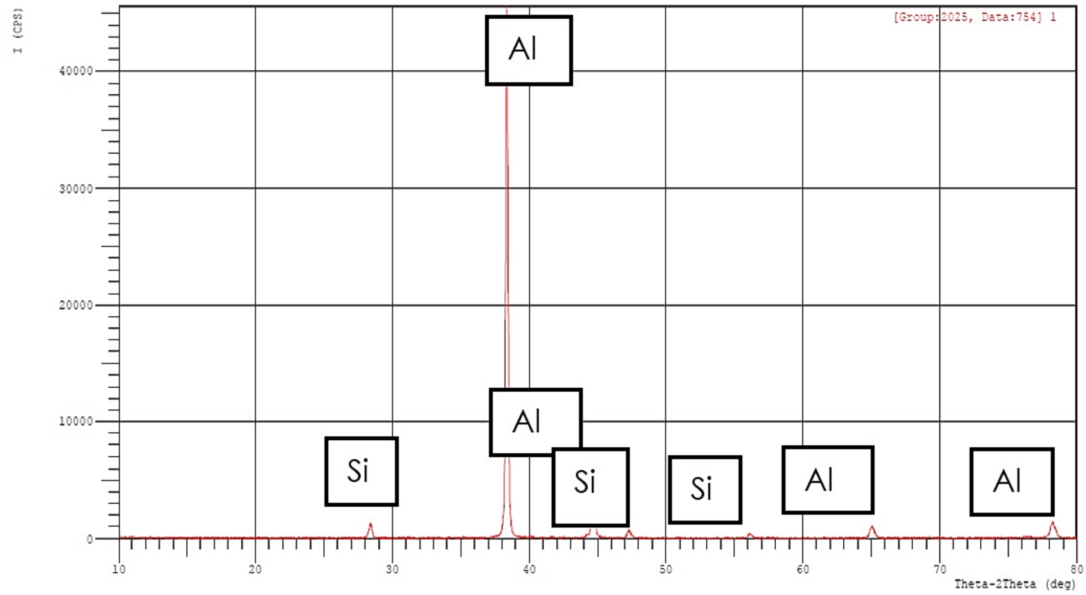

(a)

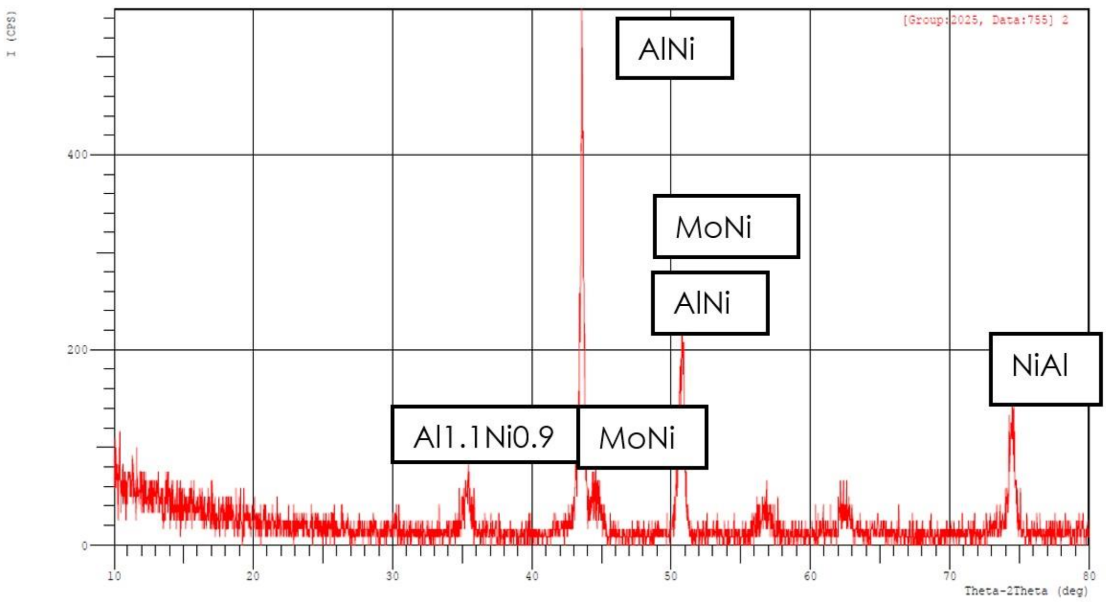

(b)

Fig. 3. XRD analysis of the (a) substrate Al alloy and (b) coating material (NiAlMo)

The substrate maintained its original metallurgical structure before coating, as evidenced by the lack of new reaction products [21]. On the other hand, the coated specimen's diffraction pattern (Fig. 3b) shows the production of many intermetallic phases, such as NiAl, $AlNi_3$, and MoNi, together with trace amounts of residual metallic components. These phases resulted from the extraordinarily high temperatures generated during plasma spraying, which were followed by the molten particles' quick solidification upon contact with the substrate. These quick heat cycles encourage the diffusion of molybdenum, nickel, and aluminum, which leads to the creation of stable intermetallic complexes. NiAl is one of the main phases that strengthens the coating because of its exceptional hardness, oxidation resistance, and thermal stability [22, 23]. Similarly, MoNi improves the coating's resistance to abrasive wear and elevated-temperature deterioration, while $AlNi_3$'s comparatively high hardness helps to improve the mechanical integrity of the coating. These intermetallic compounds work together to form an efficient barrier against severe wear and hot corrosion and to explain the significant increase in surface hardness seen after coating. The current results are in good agreement with earlier studies on Ni-based plasma-sprayed coatings, where the main mechanism for improving hardness, wear resistance, and oxidation behavior has been found to be the production of Ni–Al intermetallic compounds. Consequently, the XRD data offer compelling proof that the development of these hard intermetallic phases during plasma spraying is directly linked to the enhanced mechanical and tribological characteristics found in this investigation.

3.3. Microhardness Measurements

The Vickers microhardness values of the plasma-sprayed NiAlMo coating and the uncoated Al–Si substrate are shown in figure (4). The untreated Al–Si substrate had an average microhardness of 103.7 HV, while the NiAlMo coating showed a significantly greater microhardness of 347 HV. The creation of hard intermetallic phases, specifically NiAl, $AlNi_3$, and MoNi, as determined by XRD investigation, is the main cause of this significant rise. These phases offer an efficient load-bearing surface during indentation because they are significantly harder than the aluminum matrix. Furthermore, by limiting localized plastic deformation, the improved lamellar microstructure created by the quick solidification linked to atmospheric plasma spraying strengthens the coating even more. The strong metallurgical integrity of the deposited coating is another significant feature that contributes to the hardness improvement. The SEM cross-sectional observations show that the coating has a dense structure with low porosity and high adherence to the substrate. These features enable the coating layer to efficiently support the imposed load during the hardness test instead of transferring it to the comparatively soft aluminum substrate [24].

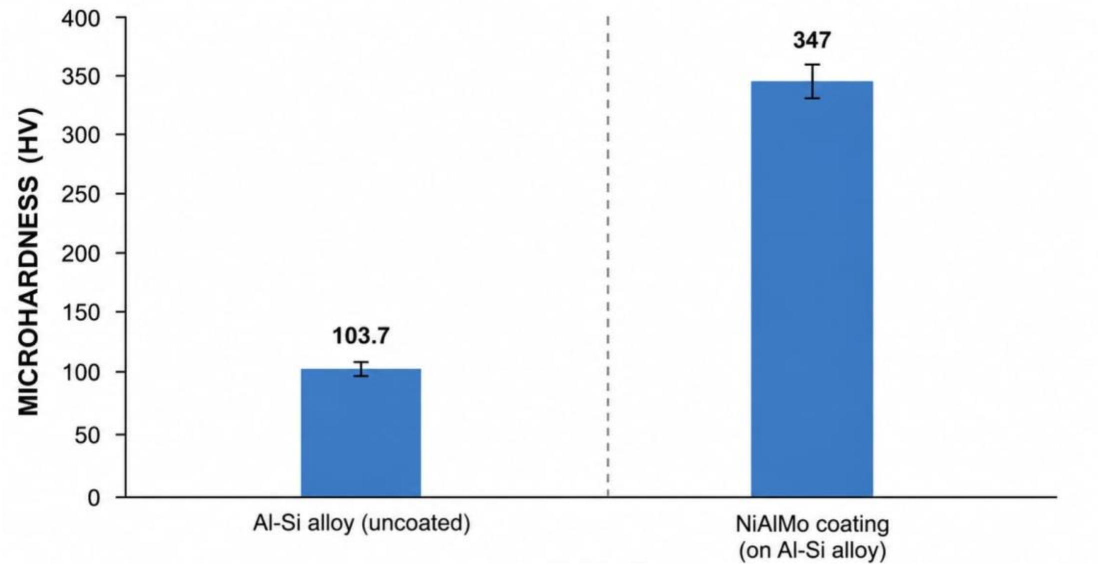

Fig. 4. Vickers microhardness measurements of the investigated study

3.4. Wear Test

A 20 mm-diameter cylindrical pin was used for the wear tests. Under the same testing settings, three standard loads of 5, 10, and 15 N were applied. The pin's nominal contact area was 314.16 mm^2. Consequently, 0.0159, 0.0318, and 0.0477 MPa were the corresponding normal contact pressures.

The results of the wear rate clearly explain the influence of the coating on improving the wear resistance of the aluminum alloy. A comparison between the coated and uncoated samples reveals a massive reduction in wear rate after applying the coating, as shown in Figure (5) [25,26]. For the uncoated samples, the wear rate increased gradually with increasing applied load. At 5 N, the wear rate was 1.90×10^{-5} g/m, which increased to 3.81×10^{-5} and 5.71×10^{-5} g/m at 10 and 15 N. These trends indicate that heavier loads increase material removal due to increased contact stress and frictional forces at the sliding interface. In contrast, the coated samples exhibited much lower wear rates under the same testing conditions. The wear rate values were 4.08×10^{-6}, 8.17×10^{-6} and 1.23×10^{-5} g/m at 5 N, 10 N, and 15 N, respectively. This significant decrease confirms the effectiveness of the coating in enhancing surface properties. The findings show that multiple factors significantly influence the wear rate. The initial factor pertains to the development of loads from 5 to 15 Newtons, resulting in an increased wear rate. The second factor, a reduction in wear rate from applying a hard surface layer, created challenges in removing the metal from the surface, thereby improving the material's surface properties.

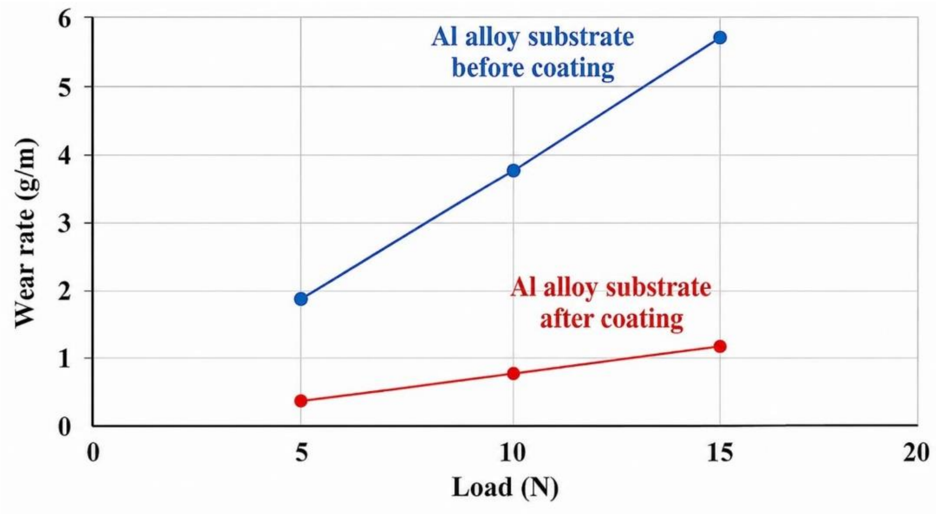

Fig. 5. Wear rate relation with load for the current study

Before coating **After coating**

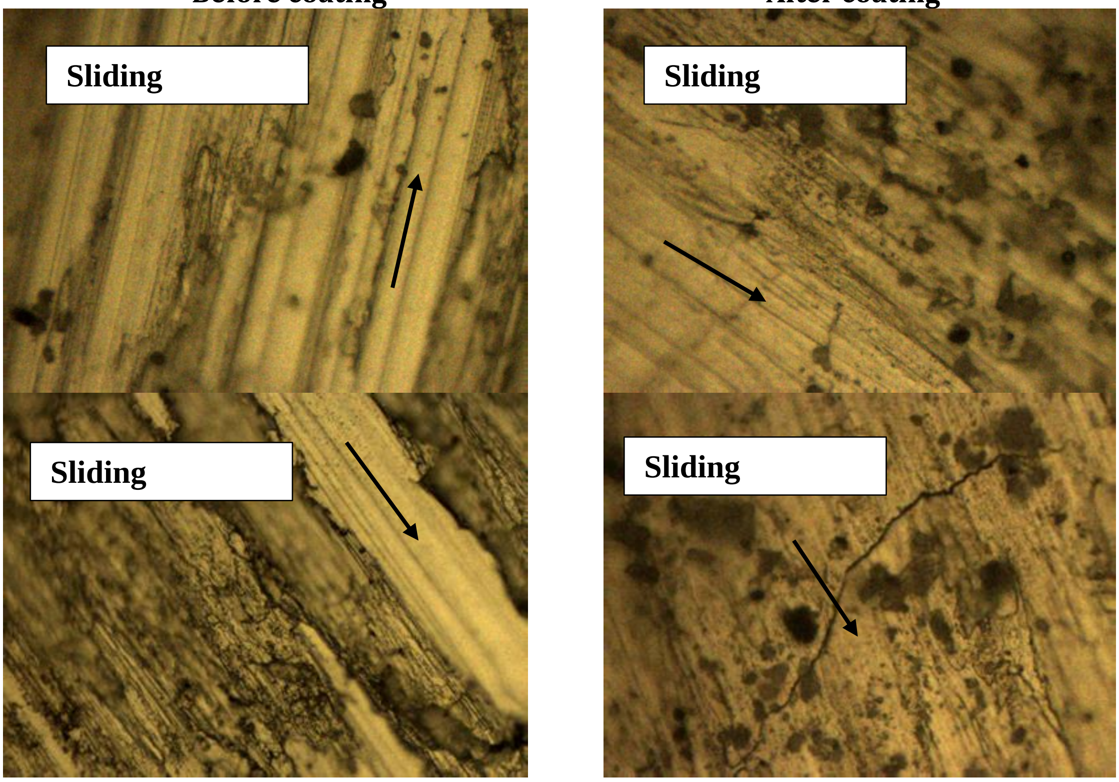

5N

10N

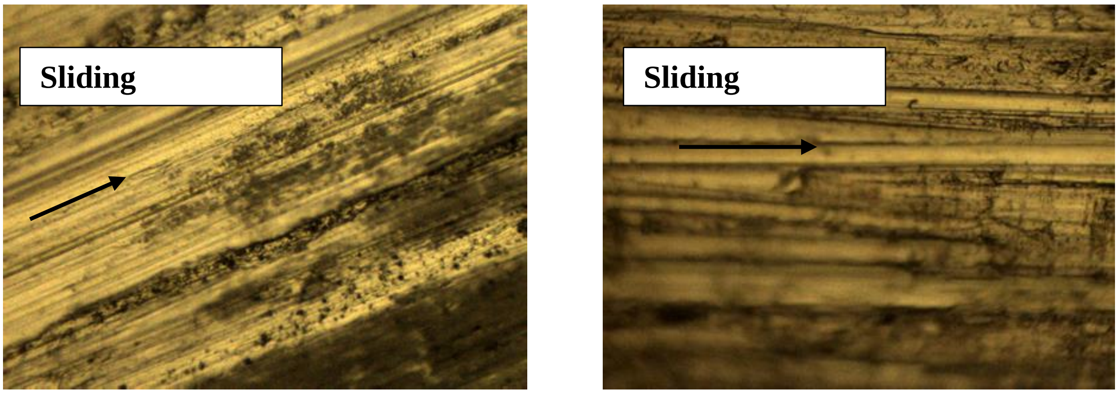

15N

Fig. 6. Optical microscope images of the wear track for Al alloy before and after coating using NiAlMo at 40X magnification

The left side of Fig. 6 presents optical microscope images illustrating the wear track of the uncoated Al alloy substrate, where the presence of deep grooves and plough marks indicates a higher wear rate relative to the coated sample's wear track [27]. In contrast, the right of Fig. (6) shows that the grooves and plough marks are narrower, with reduced width and shallower valleys, attributable to the resistance against indentation by the sliding disk on the pin. The plough marks and micro-scratch lines generally diminish in thickness with the application of the coating layer. The scratch lines are exceptionally thin and narrow due to the increased hardness of the coating materials NiAlMo, as illustrated in Figure (6). Generally, the grooves increase in thickness with the applied load in both instances.

3.5. Corrosion Test

The test included three samples:

- A coated sample without surface finishing (Sample 1),
- A coated sample with surface finishing (Sample 2),
- An uncoated, surface-finished sample (Sample 3).

The extent of corrosion was evaluated based on weight change, calculated according to;

$$\Delta W = Initial\ Weight\ (Wi) - Final\ Weight\ (W_f) \quad (1)$$

As commonly reported in recent hot corrosion studies [28]. The findings for Sample 1 and Sample 2 indicate significant resistance to both corrosion and oxidation. The corrosion rate of the coated aluminum substrate in the presence of mixed salts (Na_2SO_4 and V_2O_5) is linear, as shown in Figure (7a). These samples exhibited thermal stability, which is attributed to the NiAlMo coating. The coating layer serves as a barrier against oxygen infiltration through its thickness [29], thereby preventing the formation of an oxidation layer on the surface of the aluminum alloy.

Sample 3 also showed an increase in weight (+0.001 g), indicating the oxidation of the aluminum alloy and the formation of an aluminum oxide layer. However, the durability of this protective layer is expected to be less than that of the coated sample. At cycle 10, the sample weighed 5.3726 grams, and at cycle 50, it weighed 5.3736 grams. The protective oxide layer may deteriorate, leading to increased corrosion and an accelerated rate of aluminum degradation, as illustrated in the Figure(7b). Therefore, it is essential to investigate protective coatings or treatments that may mitigate these detrimental effects and extend the durability of aluminum components in these conditions.

Figure (7) shows the SEM images and EDS analysis of the upper surface of the samples to observe the sample-layer elements' distribution. The results showed a clear difference of chemical composition between the coated and uncoated samples. For samples 1 and 2 the composition includes these elements: Al, Si, Ni, Mo, O, N, and V, which corresponds to the chemical composition of the Al alloy with coating layer that composed from (NiAlMo) as well as to the corrosion salt that contains V. While the Al alloy sample without coating (Sample 3) is composed of Al, Si, O, N, and V which corresponds to the chemical composition of the Al alloy with corrosion salts that contains V Table (3).

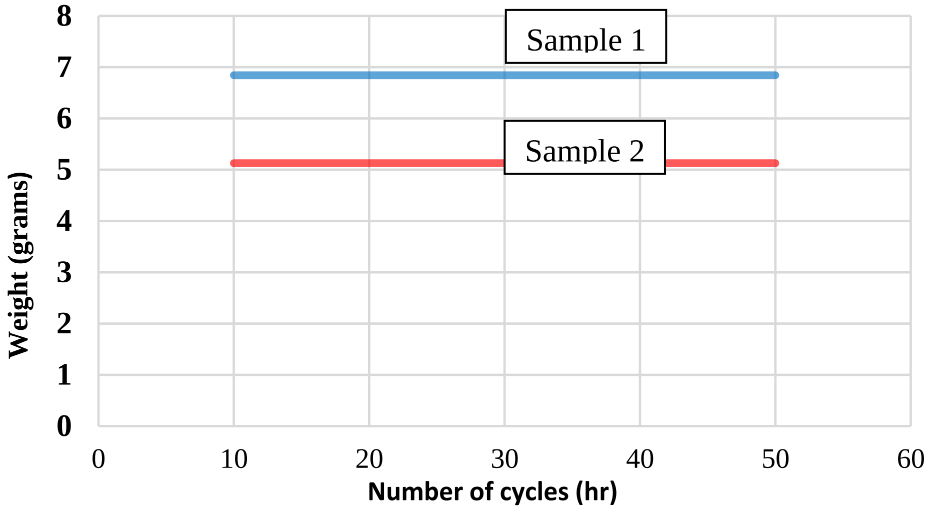

(a)

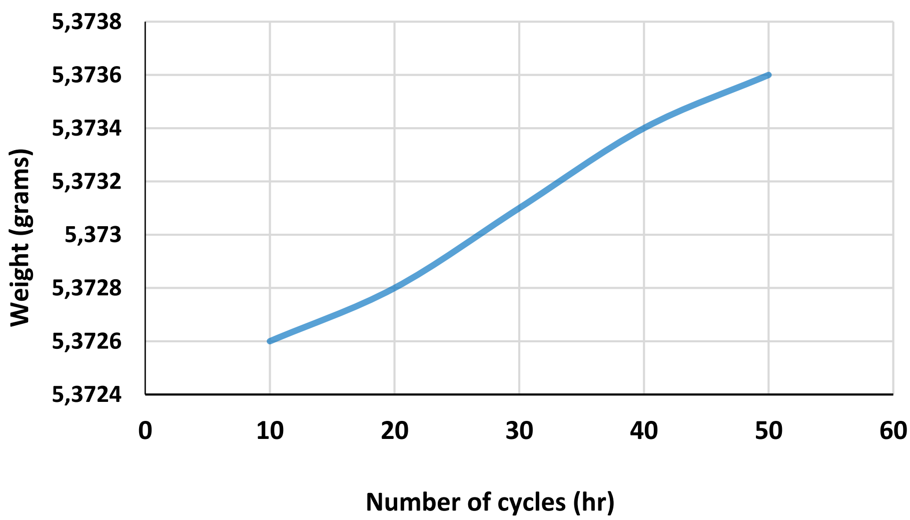

(b)

Fig. 7. (a) Coated Al alloy with NiAlMo—weight vs. number of cycles (b) Uncoated Al alloy - weight v/s number of cycles

Table 3. EDS of the substrate material and NiAlMo coating in hot corrosion

Element	Sample 1 weight%	Sample 2 weight%	Sample 3 weight%
Al	71.7	63.2	66.6
Si	13.4	19.1	17
O	12.1	15	13.6
Ni	0.9	0.8	0
V	0.3	0.8	1.7
Mo	1.4	1.2	0
N	0.4	-	1.1

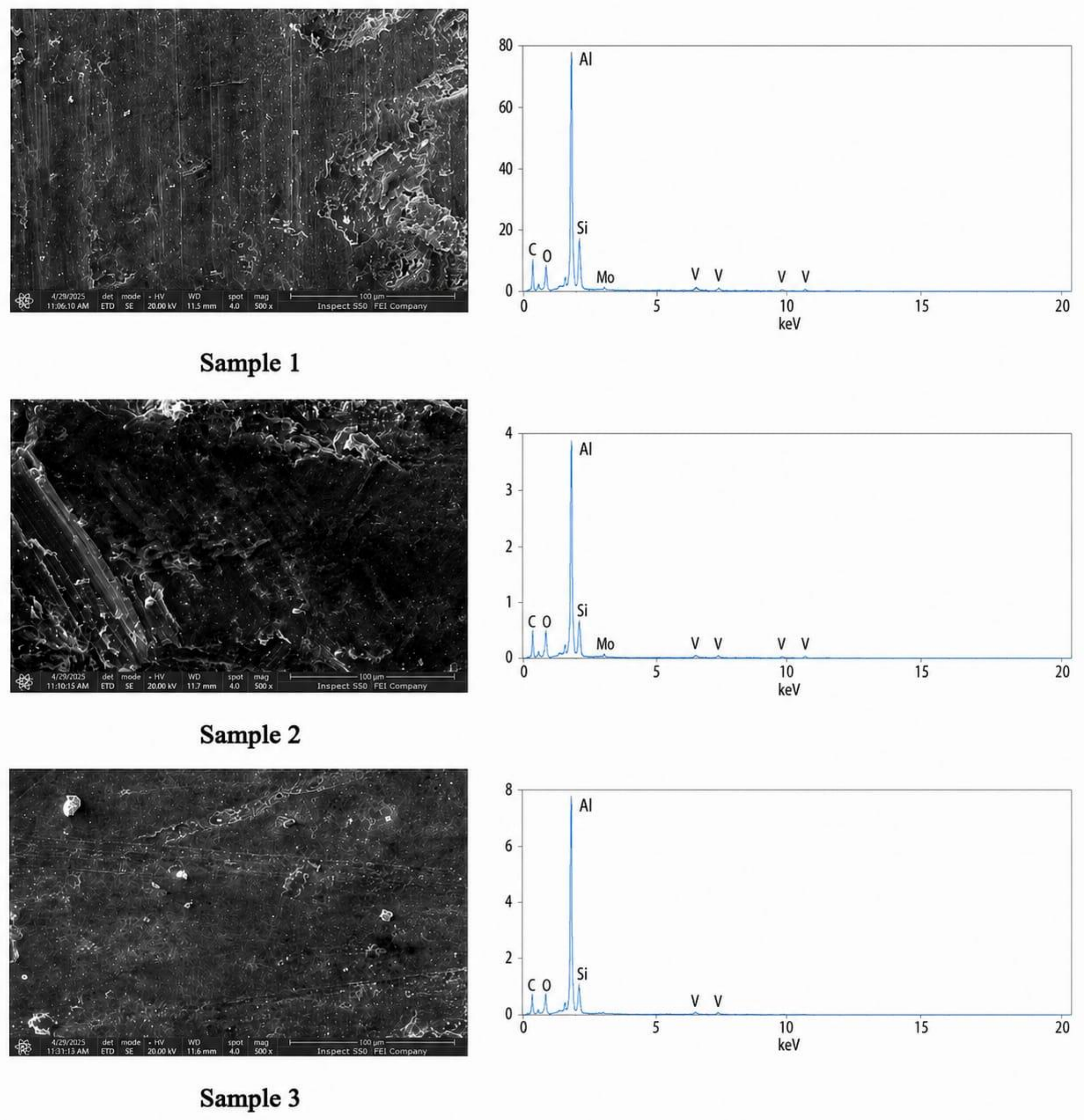

Fig. 8. The SEM images and EDS analysis display the identified elements

4. Conclusions

- In this work, a NiAlMo coating was successfully applied via atmospheric plasma spraying to enhance the surface characteristics of a hypereutectic Al–Si piston alloy. The deposited coating had an average thickness of around 600 μm and a dense lamellar microstructure that adhered well to the aluminum substrate. The production of intermetallic phases, such as NiAl, $AlNi_3$, and MoNi, was confirmed by XRD analysis. These phases significantly enhanced the coated alloy's mechanical and tribological performance.
- The plasma-sprayed NiAlMo coatings consist of a heterogeneous grain size distribution ranging from 0.5 to 4 μm.
- The coated specimen's microhardness improved by about 235%, from 103.7 HV for the bare substrate to 347 HV following coating. The development of hard intermetallic phases and the refined lamellar coating structure created during plasma spraying were primarily responsible for this improvement.
- The NiAlMo coating considerably decreased the wear rate under all applied loads (5, 10, and 15 N), according to the wear test results. Because the hard coating successfully withstood

abrasive wear and plastic deformation, the coated specimens continuously showed less material loss than the uncoated alloy. The coated specimens had shorter grooves and less severe surface damage, indicating better tribological performance, according to SEM studies of the worn surfaces.

- The coated specimens had significantly greater corrosion resistance than the uncoated substrate, according to a hot corrosion test conducted in a molten salt environment containing 55 weight percent V_2O_4 and 45 weight percent Na_2SO_4 at 350°C for 50 hours. The production of protective oxide layers and stable nickel–aluminum intermetallic compounds, along with the dense coating structure, significantly inhibited material deterioration during exposure and prevented corrosive species from penetrating.
- Overall, the experimental findings show that atmospheric plasma-sprayed NiAlMo coatings offer a practical surface engineering approach for enhancing the Al–Si piston alloys' hardness, wear resistance, and hot corrosion behavior without changing the substrate's bulk characteristics. Therefore, the suggested coating technique has a great deal of potential to increase the longevity and dependability of lightweight automobile engine parts operating in harsh mechanical and thermal environments. Future research could concentrate on assessing the coated alloy's fatigue performance, high-temperature oxidation behavior, and long-term durability under circumstances that more closely resemble real-world engine operation.

References

[1] Dada M, Popoola P. Recent advances in joining technologies of aluminum alloys: a review. Discov Mater. 2024;4:86. https://doi.org/10.1007/s43939-024-00155-w

[2] Sharma S, Kumar R, Dutta PK. A comparative review on thermal spray coatings for aluminum alloy substrates: Challenges and opportunities. Surf Coat Technol. 2023;465:129602.

[3] Gupta M, Sinha SK, Sharma RK. Enhancing wear and corrosion resistance of Al-Si alloy using HVOF sprayed WC-10Co-4Cr coating: Parametric optimization and characterization. J Mater Res Technol. 2022;19:4293-4307.

[4] Jenny MP, Kabecha WW. Advantages and Challenges of Implementing Lightweight Materials in Automobiles: A Review. Int J Sci Res Publ. 2023;13(9):14116. https://doi.org/10.29322/IJSRP.13.09.2023.p14116

[5] Kumar P, Srivastava VK, Sharma A. Influence of cooling mediums on mechanical and tribological characteristics of Al/Cu-based composites reinforced with chromium particles. Tribol Mater. 2025;4(3):134-143. https://doi.org/10.46793/tribomat.2025.016

[6] Vencl A, Rac A, Bobić I, Mišković Z. Tribological Properties of Al-Si Alloy A356 Reinforced With Al_2O_3 Particles. Tribol Ind. 2006;28(1-2):27-31.

[7] Ang HQ, Kumar G, Karakulak E. Development of Light Alloys and Their Applications. Crystals. 2026;16(1):11. https://doi.org/10.3390/cryst16010011

[8] Cui L, Liu K, Chen XG. Recent advances in cost-effective aluminum alloys with enhanced mechanical performance for high-temperature applications: A review. Mater Des. 2025;253:113869. https://doi.org/10.1016/j.matdes.2025.113869

[9] Sadeghi E, Markocsan N, Joshi S. Advances in Corrosion-Resistant Thermal Spray Coatings for Renewable Energy Power Plants. Part I: Effect of Composition and Microstructure. J Therm Spray Tech. 2019;28(8):1751-1788. https://doi.org/10.1007/s11666-019-00938-1

[10] Jia B, Ren R, Zhang H, Man T, Cui X, Liu T, et al. Research Advancements of Wear-Resistant Coatings Fabricated on Aluminum and Its Alloys. Coatings. 2025;15(7):750. https://doi.org/10.3390/coatings15070750

[11] NayebPashaee N, Bakhtiarifard F, Jalali M, Khodadostan A, Koohfar A, Mousavi Sorkhkolai SK, et al. High-entropy alloy coatings for surface protection and thermal barrier applications: fundamentals, recent advances, and a critical assessment of their potential as alternatives to conventional coatings. Discov Mater. 2026;6:11. https://doi.org/10.1007/s43939-025-00480-8

[12] Abbas RA, Ajeel SA, Ali Bash MA, Kadhim MJ. Effect of plasma spray distance on the features and hardness reliability of YSZ thermal barrier coating. Mater Today Proc. 2021;42:2560-2566. https://doi.org/10.1016/j.matpr.2020.12.578

[13] Xu X, Li W, Wan B, Jin S, Chen K, Su F. Extremely improved the corrosion resistance and anti-wear behavior of aluminum alloy in 3.5% NaCl solution via amorphous CrAlN coating protection. Corros Sci. 2024;230:111952. https://doi.org/10.1016/j.corsci.2024.111952

[14] Abbas RA, Ajeel SA, Ali Bash MA, Kadhim MJ. The Influence of Spray Distance on the Assessment of Porosity in YSZ Thermal Barrier Coating. AIP Conf Proc. 2022;2394(1):040003. https://doi.org/10.1063/5.0108472

[15] Vencl A, Mrdak M, Banjac M. Correlation of microstructures and tribological properties of ferrous coatings deposited by atmospheric plasma spraying on Al-Si cast alloy substrate. Metall Mater Trans A. 2009;40(2):398-405. https://doi.org/10.1007/s11661-008-9693-0

[16] Mrdak M, Vencl A. Microstructure and mechanical properties of the mo-NiCrBSi coating deposited by atmospheric plasma spraying. FME Trans. 2009;37(1):27-32.

[17] Dimitrova V, Dimitrov V, Zdravcheva G. Anodic and chrome coatings for firearm barrels: Microstructural and phase analysis. Tribol Mater. 2026;1(5):22. https://doi.org/10.46793/tribomat.2026.005

[18] Vencl A. Optimization of the deposition parameters of thick atmospheric plasma spray coatings. J Balk Tribol Assoc. 2011;18(3).

[19] Shreerama B, Rajeshwaran M, Jinnah SM, Nandhakumar S, Anil Kumar TC. Thermal analysis of functionally graded mullite - La2O3 coated aluminium alloy piston using plasma spraying. J Ceram Process Res. 2022;23(3):263-267.

[20] Kalyana Kumar M, Sudersanan PD. Experimental Study to Improve the Mechanical Properties of an Aluminum Piston for an IC Engine by Coating it with Zirconium Dioxide. J Mines Met Fuels. 2024;72(12):1371-1382. https://doi.org/10.18311/jmmf/2024/45966

[21] Biswas P, Patra S, Mondal MK. Structure-property correlation of eutectic Al-12.4 Si alloys with and without zirconium (Zr) addition. Int J Cast Met Res. 2020;33(2-3):134-145. https://doi.org/10.1080/13640461.2020.1769319

[22] Guettaf Temam E, Ben Temam H, Benramache S. Surface morphology and electrochemical characterization of electrodeposited Ni-Mo nanocomposites as cathodes for hydrogen evolution. Chin Phys B. 2015;24(10):108202. https://doi.org/10.1088/1674-1056/24/10/108202

[23] Bai Y, Zhou J, Li J, Yang Z. B_2-ordered NiAl content on microstructure, mechanical, and oxidation properties of FeAl intermetallic compounds. J Mater Res Technol. 2022;16:1875-1888. https://doi.org/10.1016/j.jmrt.2021.12.128

[24] Krim S, Giljean S, Marsiquet C, Loucif K, Pac MJ. Hardness of nickel electrodeposition on aluminum alloys: influence of temperature and duration of heat treatment. In: Proceedings of the 14th International Conference on Local Mechanical Properties; 2019.

[25] Jia B, Ren R, Zhang H, Man T, Cui X, Liu T, et al. Research Advancements of Wear-Resistant Coatings Fabricated on Aluminum and Its Alloys. Coatings. 2025;15(7):750. https://doi.org/10.3390/coatings15070750

[26] Li X, Wang K, Jiang B, Chen Y, Zhang Z, Lu K, et al. Enhancing corrosion and wear resistance of a 7075 aluminum alloy via depositing TC4 coating. J Mater Res Technol. 2024;32:1736-1748. https://doi.org/10.1016/j.jmrt.2024.08.037

[27] Nataraja M, Balakumar G, Santhosh N, Rudra Naik M. Characterization of wear rate of Al-12 wt% Si alloy based MMC reinforced with ZrO2 particulates. Mater Res Express. 2024;11(3):036522. https://doi.org/10.1088/2053-1591/ad3468

[28] Magogodi S, Mathabathe MN, Rikhotso-Mbungela R, Vilane V, Siyasiya C, Bolokang AS. The effect of hot corrosion on mechanical properties of the tin-doped titanium aluminide alloy. Int J Adv Manuf Technol. 2025;136(5-6):2623-2636. https://doi.org/10.1007/s00170-024-14935-4

[29] Ali Bash MA, Mezher Resen A, Kareem AHA, Muhi Abdulsahib Y. Improving the Hot Corrosion Behavior of Plasma-sprayed MCrAlY by RF Sputtering of TiO_2 Nano-Coating and Laser Remelting Treatment. Prog Color Colorants Coat. 2024.